JACS
JOURNAL OF THE AMERICAN CHEMICAL SOCIETY

ARTICLE

pubs.acs.org/JACS

Zinc-Bacteriochlorophyllide Dimers in de Novo Designed Four-Helix Bundle Proteins. A Model System for Natural Light Energy Harvesting and Dissipation

Ilit Cohen-Ofri,[†] Maurice van Gastel,[‡,§] Joanna Grzyb,[†,∥] Alexander Brandis,[†] Iddo Pinkas,[†] Wolfgang Lubitz,[‡] and Dror Noy*[,†]

[†]Plant Sciences Department, Weizmann Institute of Science, Rehovot 76100, Israel

[‡]Max Planck Institute for Bioinorganic Chemistry, Stiftstrasse 34-36, 45470 Mülheim an der Ruhr, Germany

ABSTRACT:

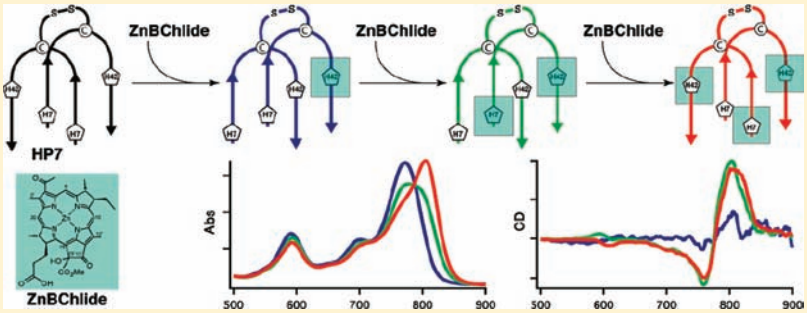

Photosynthetic organisms utilize interacting pairs of chlorophylls and bacteriochlorophylls as excitation energy donors and acceptors in light harvesting complexes, as photosensitizers of charge separation in reaction centers, and maybe as photoprotective quenching centers that dissipate excess excitation energy under high light intensities. To better understand how the pigment's local environment and spatial organization within the protein tune its ground- and excited-state properties to perform different functions, we prepared and characterized the simplest possible system of interacting bacteriochlorophylls within a protein scaffold. Using HP7, a high-affinity heme-binding protein of the HP class of de novo designed four-helix bundles, we incorporated 13^2-OH-zinc-bacteriochlorophyllide-a (ZnBChlide), a water-soluble bacteriochlorophyll derivative, into specific binding sites within the four-helix bundle protein core. We capitalized on the rich and informative optical spectrum of ZnBChlide to rigorously characterize its complexes with HP7 and two variants, in which a single heme-binding site is eliminated by replacing histidine residues at positions 7 or 42 by phenylalanine. Surprisingly, we found the ZnBChlide binding capacity of HP7 and its variants to be higher than for heme: up to three ZnBChlide pigments bind per HP7, or two per each single histidine variant. The formation of dimers within HP7 results in dramatic quenching of ZnBChlide fluorescence, reducing its quantum yield by about 80%, and the singlet excited-state lifetime by 2 orders of magnitudes compared to the monomer. Thus, HP7 and its variants are the first examples of a simple protein environment that can isolate a self-quenching pair of photosynthetic pigments in pure form. Unlike its complicated natural analogues, this system can be constructed from the ground up, starting with the simplest functional element, increasing the complexity as needed.

INTRODUCTION

Chlorophylls (Chls) and bacteriochlorophylls (BChls) are the primary light-absorbing pigments of photosynthetic organisms. Most of them are organized in densely packed arrays within light harvesting protein complexes (LHCs),[1] while a small fraction, embedded in reaction center (RC) proteins,[2] initiates and propagates photoinduced charge separation that provides the driving force for all further metabolic processes.[3] The LHCs provide a high absorption cross-section over a broad wavelength range and maintain sufficient photon flux to the RC.[4] In this architecture, known as the photosystem, interacting (B)Chls function as excitation energy donors and acceptors in LHCs, on one hand, and photosensitizers of electron transfer in RCs, on the other hand. An additional protective role for interacting (B)Chls as quenching centers that dissipate excess excitation energy under high light intensities was recently suggested.[5,6] Clearly, the pigment's local environment and spatial organization within the protein determine its functionality by tuning its ground- and excited-states properties. Yet, although the details of many natural (B)Chl−protein structures are known at high spatial resolution, and excitation energy and charge transfer processes are well understood and can be followed with high temporal resolution,[1,7−9] the complexity and

Received: March 6, 2011
Published: May 12, 2011

dx.doi.org/10.1021/ja202054m | J. Am. Chem. Soc. 2011, 133, 9526–9535

diversity of the natural systems[10,11] obscure the fundamental factors determining the balance between light harvesting, dissipation, and charge separation.

To explore the details of (B)Chl−(B)Chl and (B)Chl−protein interactions in the simplest possible system, we prepared and characterized a simple BChl−protein complex comprising a minimal number of water-soluble BChl derivatives bound to a de novo designed protein. We chose to use the well-established HP class of de novo designed four-helix bundles that were originally developed by the Dutton lab[12−14] and has proven extremely valuable for understanding the underlying parameters of heme−protein functionality.[12,15−17] Particularly, we focused on HP7, a high-affinity heme-binding protein of the HP class, for which binding of the water-soluble zinc-substituted bacteriochlorphyllide-a (BChlide) derivative 13^2−OH−Zn−BChlide (ZnBChlide) was already demonstrated.[18] The 13^2-OH derivative was preferred over the native 13^2-H derivative because the latter is spontaneously converted into the 13^2-OH derivative in aqueous solvents. Thus, using the pure 13^2-OH derivative improves sample homogeneity. Here, we report on the incorporation of interacting ZnBChlide pigments into HP7, and two additional variants, HP7H7F and HP7H42F, in which a single heme-binding site is eliminated by replacing histidine residues at positions 7 or 42, respectively, by phenylalanine.

ZnBChlide is an excellent building block for constructing water-soluble analogues of natural LHCs because its high chemical homology and spectral properties are almost identical to those of natural BChls. Its bacteriochlorin-type optical spectrum is the richest and most informative as compared to the protoporhyrin- and chlorin-type spectra of heme, and Chl derivatives, respectively. Particularly, the well-resolved lowest energy electronic transitions, Q_x and Q_y, are excellent probes for local changes in the electronic environment as a result of pigment−pigment and protein−pigment interactions. Furthermore, the moderately absorbing Q_x transition is a direct reporter of the ligation state and charge density of the central metal.[19−23] Importantly, the coordination preferences of the central Mg atom of native BChl are very similar to zinc and very different from the native central Fe atom of heme. Thus, while bis-histidyl ligation is the most abundant heme-binding mode in heme−proteins,[24] it is rarely found in (B)Chl proteins where axial ligation by a single histidine is the preferred binding mode.[25] Similarly, monohistidyl ligation is exclusively preferred in natural and artificially reconstituted ZnBChl proteins.[20,26]

So far, very few examples of binding Chl derivatives,[27,28] and even fewer of binding BChl derivatives[29] to de novo designed proteins have been reported. This is despite the significant chemical homology of heme, Chls, and BChls, the successful introduction of (B)Chl derivatives into natural heme-binding proteins such as myoglobin,[30,31] and the great interest in the energy conversion functionalities of (B)Chls in photosynthetic enzyme complexes. The hydrophobic nature of (B)Chls and their tendency to self-aggregate in polar solvents severely limit incorporation into water-soluble proteins and require either chemically modifying the natural pigments, or working in more hydrophobic environments like lipid membranes or detergent micelles. Unfortunately, the latter condition demands the use of transmembranal-like proteins that are compatible with these environments but are much more difficult to design, control, and characterize than water-soluble proteins. Thus, despite a few successful examples of (B)Chl-binding and assembly with de novo designed hydrophobic and amphipathic protein scaffolds,[32−39] progress in this direction has been very slow.

Our spectroscopic studies reveal substantial differences between heme and ZnBChlide incorporation into HP7 and its variants. Surprisingly, we found that the proteins can adopt an alternative quaternary structure for ZnBChlide binding that was not considered for heme binding. This conformation enables binding of up to two monohistidine ligated ZnBChlide pigments each at positions 7 and 42. Consequently, HP7H7F and HP7H42F bind up to two ZnBChlide pigments per protein, whereas HP7 binds up to three pigments per protein. Binding of a fourth ZnBChlide to HP7 was not observed probably due to steric crowding. Additionally, we found that excitonic interactions are predominant between two or more protein-bound ZnBChlide molecules. These shorten the excited-state lifetime by 2 orders of magnitude, thereby leading to significant fluorescence quenching. We discuss implications of these findings for the functionality of natural LHCs and the de novo design of functional (B)Chl−protein complexes.

EXPERIMENTAL SECTION

Pigment Preparation. BChl-a (Scheme 1, **1**) was isolated from *Rhodobacter sphaeroides* using standard methods.[40] It was first hydroxylated at position C-13^2 to yield 13^2-OH-BChl-a (Scheme 1, **2**), by dissolving in methanol and stirring in the dark for 3 days. Next, the phytyl ester was hydrolyzed by dissolving in 80% TFA (trifluoro acetic acid) under Ar gas flow and stirring for 2 h. This also led to demetalation of the Mg atom and yielded 13^2-OH-bacteriopheophorbide-a (Scheme 1, **3**), as the primary product, which was purified on a silica gel column and used for ZnBChlide synthesis by the transmetalation method.[41] An excess of anhydrous cadmium acetate was added to Bacteriopheophorbide-a in refluxing dimethylformamide (DMF) under strict Ar protection and was stirred for 40 min at 110 °C. The reaction was followed spectroscopically and ran to completion. Sodium ascorbate and zinc acetate were then added to the mixture, and this reaction too was followed spectroscopically and ran to completion. The desired product, 13^2-OH-Zn-BChlide-a (Scheme 1, **4**), was purified on a C8 HPLC columnn (ACE 10), using a 40:60 acetonitrile:water mixture, at a flow rate of 5 mL min^{-1}. The eluting solution was evaporated; the pigments were redissolved in methanol that was also evaporated, and the remaining solid pigments were stored under Ar at −20 °C. Electrospray ionization-mass spectrometry of the purified product indicated a molecular ion (M^+) of 673 m/z, as expected from the molecular formula.

Protein Expression and Purification. A gene coding for the HP7 sequence was kindly provided by Prof. Ron Koder, City University of New York, New York, NY. Two variants, HP7H7F and HP7H42F, having Phe instead of His at positions 7 and 42 were prepared by point mutations to this DNA sequence. The HP7 protein and its two variants were overexpressed using pet32 plasmid containing a thioredoxin (Trx) tag with a TEV cleavage site in *E. coli* bl21(DE3) by standard procedures. The His_6-Trx-HP7 fusion protein was purified from the water-soluble protein fraction of the cell lysate on a HisTrap column (GE Healthcare), digested overnight at room temperature with TEV (TEV:protein ratio 1:30, 25 mM Tris/HCl pH 7.5, 0.5 mM EDTA, 1 mM DTT, 0.01% Triton) to release the 7 kDa HP7 from the 18 kDa His_6-Trx. Pure HP7 was isolated from the mixture by passing through the HisTrap column, dialyzed against HEPES buffer (50 mM HEPES + 1 M NaCl buffer, pH 8.0), concentrated (Vivaspin concentrators, cutoff 5 kDa), and stored at −20 °C. All of the chromatographic steps were carried out at 4 °C; the elution was monitored online for absorbance at 280 nm. The purity of the protein was verified by gel electrophoresis

Scheme 1. Reaction Scheme of 13^2-OH-Zn-BChlide-a Synthesis[a]

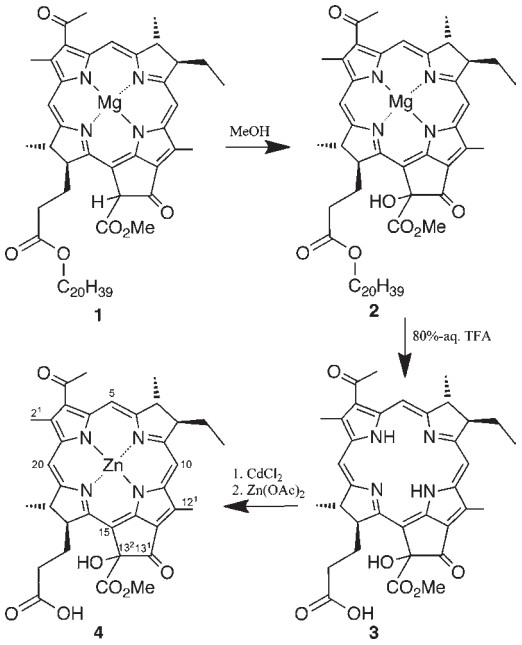

[a] BChl-a (**1**) was isolated from *Rhodobacter sphaeroides* and hydroxylated at position C-13^2 to yield 13^2-OH-BChl-a (**2**). Hydrolysis of the phytyl ester and demetalation of the Mg atom yielded 13^2-OH-bacteriopheophorbide-a (**3**), which was metalated with zinc acetate to yield the desired product, 13^2-OH-Zn-BChlide-a (**4**) (for a detailed description, see the pigment preparation section in the Experimental Section).

(Tris-Tricine SDS-PAGE, with ultra low mass marker, Sigma) and MALDI-TOF mass spectrometry.

UV−Vis−NIR Absorption and CD Spectroscopy. Absorption and CD spectra were recorded in 1 cm cuvettes on a Jasco V-7200 spectrophotometer and a Jasco J-815 spectropolarimeter, respectively. Typically, proteins at concentrations between 5 and 15 μM in HEPES buffer were titrated with concentrated methanol solutions of ZnBChlide. Protein and pigment concentrations were determined spectroscopically. The apoprotein's extinction coefficient ε_{281} = 22 mM^{-1} cm^{-1} was calculated from the amino-acid sequence by using the public domain software Sednterp[42] (http://jphilo.mailway.com/download.htm). ZnBChlide's stock concentration was determined by a four- to five-point calibration curve in phosphate buffer pH = 8, based on the pigment's peak absorption at 760 nm, using ε_{760} = 39 mM^{-1} cm^{-1}. This extinction coefficient was determined by correlating the absorption spectra of samples in diethylether with the aqueous buffer solutions, using an extinction coefficient of ε_{770} = 63 mM^{-1} cm^{-1} for ZnBChlide in diethylether.[20]

Analysis of Titration Data. Binding isotherms reflecting variations in absorption spectra were constructed by plotting second derivative values at the peak positions of the Q_x and Q_y absorption bands, and the lowest-energy exciton of Q_y versus total ZnBChlide concentration or ZnBChlide/protein ratio. Similarly, additional isotherms were constructed to reflect variations in CD spectra by using the difference between peak minima and maxima of the split Q_x and Q_y CD band. In HP7H7F and HP7H42F, the Q_x CD bands were not split; hence values of peak minimum and maximum, respectively, were used. All of the isotherms of a given protein were globally fitted to a binding equilibrium model assuming stepwise binding of ZnBChlide whereby the concentrations of free ZnBChlide, and the apoprotein, HP, can be determined, respectively, from the Adair equation:[43]

$$\frac{T_{\mathrm{ZnBChlide}} - [\mathrm{ZnBChlide}]}{T_{\mathrm{HP}}} = \frac{\sum_{i=1}^{n} i\beta_i[\mathrm{ZnBChlide}]^i}{\sum_{i=0}^{n} \beta_i[\mathrm{ZnBChlide}]^i} \quad (1)$$

and the mass balance law:

$$T_{\mathrm{HP}} = [\mathrm{HP}](1 + \sum_{i=1}^{n} \beta_i[\mathrm{ZnBChlide}]^i) \quad (2)$$

where $T_{\mathrm{ZnBChlide}}$ and T_{HP} are the total concentrations of ZnBChlide and protein, respectively, and n is the total number of binding sites per protein; $\beta_i = K_1K_2...K_i$, where K_i is the binding constant for the ith ZnBChlide given by

$$K_i = \frac{[\mathrm{HP} - \mathrm{ZnBChlide}_i]}{[\mathrm{HP} - \mathrm{ZnBChlide}_{i-1}][\mathrm{ZnBChlide}]} \quad (3)$$

The concentrations of all protein-bound ZnBChlide species are then determined from eq 3, and the observed signal, S_j, at the jth titration step of each isotherm is

$$S_j = e_f[\mathrm{ZnBChlide}] + \sum_{i=1}^{n} e_i[\mathrm{HP} - \mathrm{ZnBChlide}_i] \quad (4)$$

where e_f and e_i are proportionality constants.

The model was implemented in Igor 6.2 software (Wavemetrics Inc.), and the data were fitted using Igor's built in global fitting setup having K_i as global fitting parameters, and e_f and e_i as local parameters.

Fluorescence Spectroscopy. Fluorescence spectra and lifetime measurements were recorded on a Fluorlog-3 spectrophotometer (Horiba) and its time-corrected single-photon-counting (TCSPC) accessory, respectively. To minimize inner filter effects, a 3 × 3 mm cuvette was used for the fluorescence spectra measurements, and the sample's absorbance did not exceed 0.1. For fluorescence lifetime measurements, which required more intense fluorescence signals, a 1 cm cuvette was used, and the sample's absorbance did not exceed 0.2. A 590 nm NanoLED (Horiba) was used for generating excitation pulses with a full width at half-maximum of 1.1 ns. The emission monochromator was centered at 790 nm and set to the maximum bandwidth of 16 nm. Each decay curve consisted of 3000 photon counts and was analyzed using Horiba's DataStation v2.4 software.

Femtosecond Transient Absorption Spectroscopy. The optical system for measuring transient absorption spectra at femtoseconds to nanoseconds range was described elsewhere.[44] Samples of protein-free ZnBChlide and HP7−ZnBChlide complexes in buffer solution were pumped at their Q_x absorption band with 120 fs laser excitation pulses at 525 or 590 nm. The optical densities of the samples (in 4 and 2 mm optical path length cuvettes) were kept between 0.2 and 0.5 at the excitation wavelength.

Electron Paramagnetic Resonance (EPR). Q-band pulsed EPR and Davies ENDOR experiments were performed at T = 10 K on a Bruker ELEXYS SuperQ FT-EPR system at 34 GHz, equipped with an Oxford CF935 flow cryostat with an optical window for illumination and a home-built ENDOR resonator.[45,46] In the Davies ENDOR experiments, the first π pulse had a length of 300 ns, corresponding to an excitation bandwidth of 0.06 mT, and the length of the RF pulse was 18 μs. A Hahn echo detection sequence of 80−400−160 ns was used for the ENDOR experiment. Samples were excited in situ with an Opotek OPO laser with 7 mJ/pulse at 590 nm, pumped by a Vibrant Nd:YAG laser at a 10 Hz repetition rate.

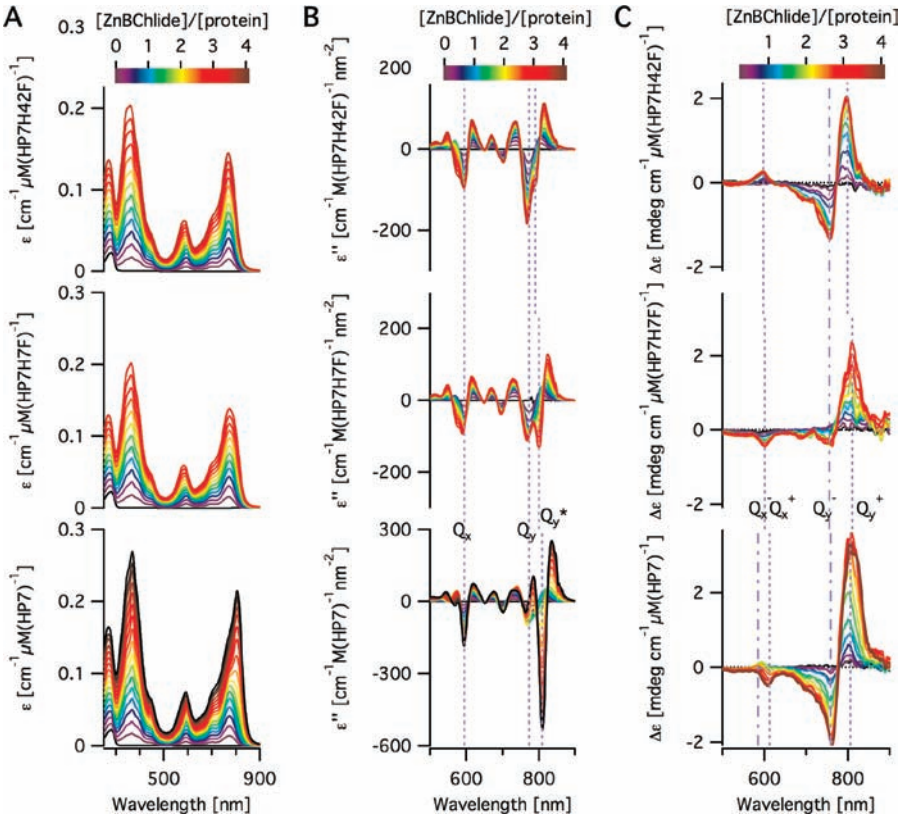

Figure 1. Titrations of ZnBChlide into 10 μM buffer solutions of HP7 (bottom), HP7H7F (middle), and HP7H42F (top) monitored by absorption (A), second derivative absorption (B), and CD spectra (C). Absorption and CD signals are per μM protein. Spectra are color-coded according to ZnBChlide:protein ratio. The vertical lines on the second derivative and CD spectra mark the positions used for constructing the binding isotherms in Figure 3.

RESULTS

ZnBChlide Incorporation into HP7, HP7H7F, and HP7H42F Proteins. Titration of a 1.1 mM methanolic solution of ZnBChlide into 10 μM buffer solutions of HP7, HP7H7F, or HP7H42F resulted in immediate incorporation of ZnBChlide into the protein as evidenced by the emergence of distinct UV−vis−NIR absorption spectra (Figure 1A). The Q_x and Q_y bands peaking at 592 and 773 nm, respectively, were the most apparent markers for ZnBChlide binding. These were significantly red-shifted from the respective 569 and 764 nm absorption peaks of ZnBChlide in a protein-free buffer. The Q_x band position is typical of ZnBChlide coordinated by a single nitrogenous axial ligand,[20,21] suggesting a role for histidine residues in the binding.

The ZnBChlide binding capacity of HP7 and its variants appears to be more than one pigment per protein. At ZnBChlide:protein ratios higher than 1:1, significant changes in the shape of the Q_y absorption band occur, accompanied by the development of unique CD spectra (Figure 1C). Second derivative absorption spectra (Figure 1B) reveal that the Q_y band is split into two new bands Q_y and Q_y*. These features are typical of excitonically interacting BChls. Representative CD and second derivative absorption spectra of the various ZnBChlide species observed during the titrations are presented in Figure 2. Notably, the peak positions of the new excitonic absorption bands (Table 1), as well as the lineshapes and intensities of their respective CD bands, vary significantly for ZnBChlide bound to HP7, HP7H7F, or HP7H42F. Furthermore, these are clearly distinguished from the spectra of ZnBChlide self-aggregates (not shown) in which the Q_y absorption band is further red-shifted to 820 nm, and the sign of its respective CD bands is reversed. Because of the water solubility of the ZnBChlide, self-aggregates of this type could be avoided in our measurements. Globally fitting selected binding isotherms of ZnBChlide titrations to a stepwise binding model (Figure 3) yielded the binding stoichiometries and dissociation constants of ZnBChlide to the proteins (Table 1). These reveal several interesting trends that distinguish ZnBChlide from heme binding:

- HP7 is capable of binding up to three ZnBChlide pigments per four-helix bundle, whereas the histidine knockout variants are capable of binding up to two pigments per bundle. This is in contrast to heme-binding capacities of two pigments in HP7 and one in its single histidine variants.
- The dissociation constants of the third ZnBChlide in HP7 and of the second in HP7H7F and HP7H42F are significantly higher than the respective dissociation constants of the first and second ZnBChlide binding to HP7. HP7H7F has the lowest binding affinity to a second ZnBChlide, whereas the affinities of HP7 and HP7H42F for a third and second ZnBChlide, respectively, are very similar.
- The affinity for each of the first two ZnBChlide molecules in HP7 is higher than the affinity for a single pigment in HP7H7F and HP7H42F. This suggests a role for histidines in stabilizing the HP7−ZnBChlide complex, in addition to the direct ligation of ZnBChlide.

dx.doi.org/10.1021/ja202054m |J. Am. Chem. Soc. 2011, 133, 9526–9535

HP7 was originally designed and shown to bind two heme cofactors, each of which was ligated by two histidine residues at positions 7 and 42. Because ZnBChlide is most probably ligated by only a single histidine, additional binding conformations become accessible, which increases the binding capacity of HP7 and its variants. A detailed analysis of the possible binding conformations is provided in the Discussion.

Steady-State Fluorescence. The fluorescence emission peak of ZnBChlide in aqueous buffer is at 796 nm, and its Stokes shift is 526 cm^{-1}. In HP7-bound ZnBChlide, the emission peak is blue-shifted to 793 nm, and the Stokes shift is dramatically reduced to 309 cm^{-1} (Table 1). This value is typical of BChl in polar organic solvents such as methanol[47] and thus indicates incorporation of ZnBChlide into the hydrophobic core of the four-helix bundle. In HP7H7F and HP7H42F, the Stokes shift decreases to 182 and 215 cm^{-1}, respectively. These changes are consistent with the expected decrease in the polarity of the four-helix bundle core upon replacing a polar histidine residue by a nonpolar phenylalanine.

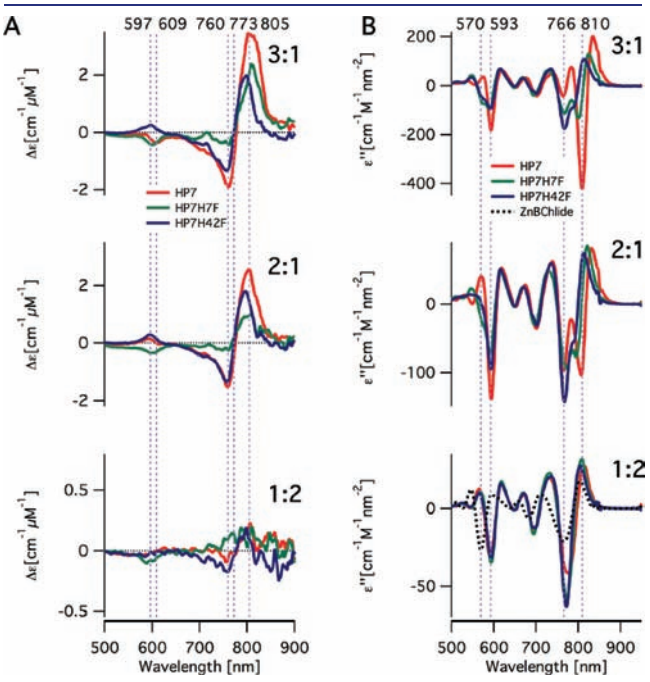

Figure 2. CD (A) and second derivative absorption spectra (B) of ZnBChlide complexes with HP7, HP7H7F, and HP7H42F in ZnBChlide:protein mixtures of 1:2, 2:1, and 3:1 molar ratios. All proteins bind a single ZnBChlide per four-helix bundle, and ZnBChlide dimers at molar ratios of 1:2 and 2:1, respectively. HP7 is the only protein capable of binding a third ZnBChlide at a molar ratio of 3:1. The second derivative absorption spectrum of unbound ZnBChlide is shown in the bottom panel (dotted line). The emergence of unbound ZnBChlide in the ZnBChlide:protein mixtures is clearly observed by its unique Q_x band at 570 nm. For easier comparison of spectral band positions, vertical lines are drawn at 597, 609, 760, 773, and 805 nm on the CD spectra and 570, 593, 766, and 810 nm on the second derivative absorption spectra.

Fluorescence Yield and Lifetime. The effects of mutual interactions between two protein-bound ZnBChlide pigments were tested by titrating 340 μM methanolic solution of ZnBChlide into 5 μM buffer solutions of HP7 (Figure 4). Emission was monitored with two excitation wavelengths, 570 and 596 nm, to selectively excite free and bound ZnBChlide, respectively. Clearly, substantial quenching of the fluorescence intensity was observed at ZnBChlide:HP7 molar ratios from 1:1 to 2:1. For excitation at 596 nm, ZnBChlide emission reached a minimum at the 2:1 molar ratio and leveled off at higher molar ratios. In contrast, the emission intensity for excitation at 570 nm began rising again at molar ratios higher than 2:1. Similar titrations of HP7H7F and HP7H42F revealed no indication of quenching; the emission intensity leveled off at ZnBChlide:protein ratios over 1:1 when samples were excited at 596 nm but kept increasing when samples were excited at 570 nm. These trends are consistent with binding two ZnBChlide molecules per HP7, and only one per HP7H7F and HP7H42F, which is reasonable considering the dissociation constants of the third ZnBChlide in HP7 and the second one in HP7H7F and HP7H42F (Table 1) are higher than the protein concentration in the measured samples. Indeed, the excitation spectra of ZnBChllide in all three proteins reflect the absorption features of bound pigments at molar ratios of 1:1, free pigments at 3:1, and intermediate features at 2:1 (Figure 4B). Notably, the overall intensity of ZnBChlide in HP7 is much lower as compared to the other two variants at higher than equimolar ratios as a result of the self-quenching in bound ZnBChlide pigments.

To further explore the influence of pigment−pigment interactions on their singlet-excited states, we repeated the titrations above while monitoring the fluorescence decay by time-correlated single-photon-counting (TCSPC). As controls, we performed the same measurements for ZnBChlide in methanol and in aqueous buffer. These were found to decay monoexponentially with lifetimes of 2.2 and 1.2 ns, respectively. Under conditions where HP7 is expected to bind a single ZnBChlide per four-helix bundle, fluorescence decay curves were similar to ZnBChlide in methanol but were best fitted with two exponentials: the primary

Table 1. Spectral and Binding Properties of ZnBChlide and Its Complexes with HP7, HP7H7F, and HP7H42F

			absorption peaks (nm)		CD min, max, zero (nm)		emission	
protein:ZnBChlide		K_d (μM)	Q_x	Q_y	Q_x	Q_y	peak (nm)	Stokes shift (cm^{-1})
unbound	0:1		569	764			796	526
HP7	1:1	0.0050 ± 0.0001	592	774			793	309
	1:2	0.080 ± 0.001	594	766, 807	614, 591, 600	763, 805, 776		
	1:3	8.5 ± 0.2	594	764, 809	611, −, −	758, 803, 781		
HP7H7F	1:1	1.9 ± 0.3	593	773			784	182
	1:2	22 ± 9	594	770, 800	601, −, −	753, 806, 773		
HP7H42F	1:1	1.24 ± 0.04	594	773			785	215
	1:2	7.7 ± 0.5	594	767, 794	−, 597, −	758, 794, 772		

dx.doi.org/10.1021/ja202054m |J. Am. Chem. Soc. 2011, 133, 9526–9535

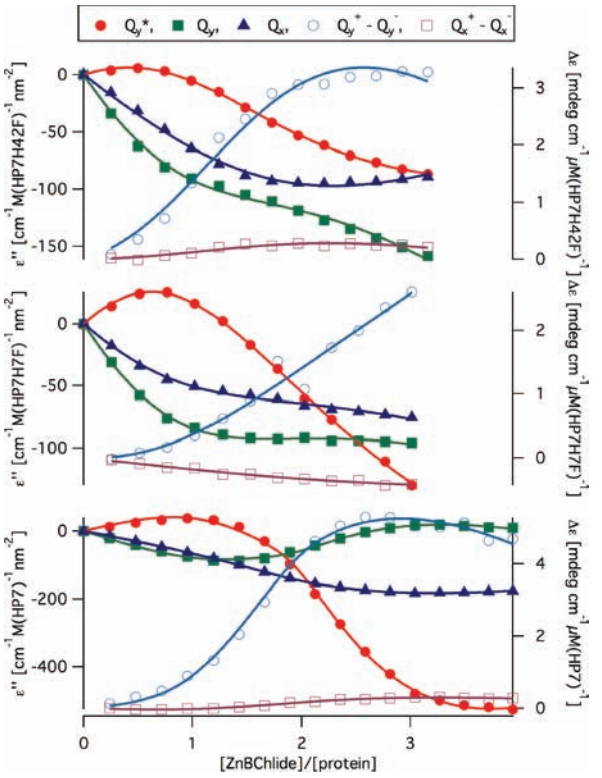

Figure 3. ZnBChlide binding isotherms of HP7 (bottom), HP7H7F (middle), and HP7H42F (top). Curves were constructed to reflect variations in peak absorption (left axis) and CD (right axis) of the monomeric and excitonically split Q_x and Q_y bands. The wavelength positions are marked in Figure 1. Q_y* is the position of the lowest-energy exciton of the Q_y absorption bands; Q_x^- and Q_x^+ and Q_y^- and Q_y^+ are the peak minima and maxima positions of the split Q_x and Q_y CD bands, respectively. Because the Q_x CD bands of HP7H7F and HP7H42F were not split, only the peak minima and maxima were considered, respectively.

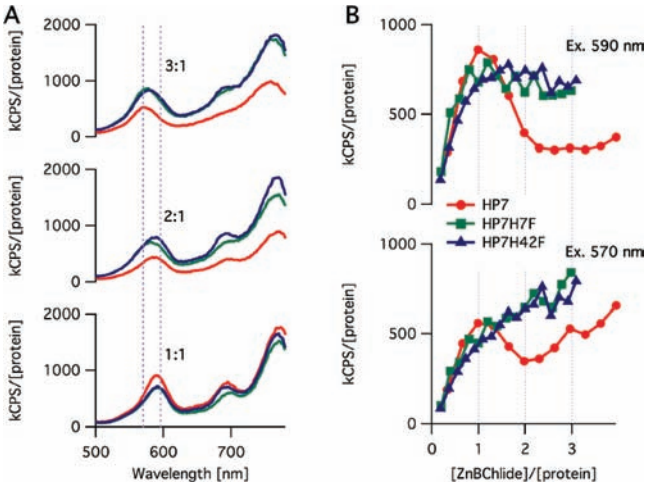

Figure 4. (A) Titrations of ZnBChlide into 5 μM buffer solutions of HP7, HP7H7F, and HP7H42F monitored by emission intensity at 790 nm upon excitation at 590 and 570 nm. (B) Fluorescence excitation spectra at selected ZnBChlide:protein molar ratios.

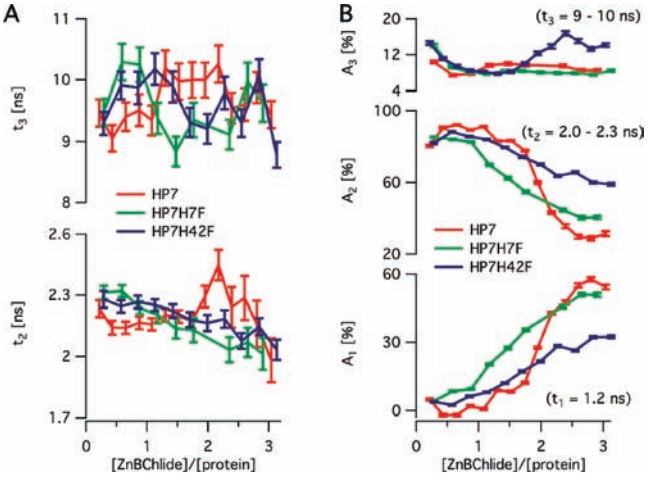

Figure 5. Exponential decay time constants (A) and their respective relative amplitudes (B) obtained from fitting fluorescence decay curves from titrations of ZnBChlide into 5 μM solutions of HP7, HP7H7F, and HP7H42F. All experimental curves were fitted with three-exponential decay curves such that one time constant, t_1, was fixed at 1.2 ns, and two constants, t_2 and t_3, were variable. The vertical error bars mark the uncertainties in fit parameters.

component with a lifetime of 2.2 ns, and a minor component (<20%) with a longer lifetime on the order of 10 ns. The latter may be attributed to contamination of Chl species that typically decay with lifetimes on the order of 6 ns[48] and instrumental artifacts. The similar lifetimes of protein-bound and unbound ZnBChlide complicate the fluorescence decay analysis of ZnBChlide:protein mixtures from titrations of HP7, HP7H7F, and HP7H42F. To better resolve the relative contributions of free and bound ZnBChlide to the overall fluorescence decay, curves from all ZnBChlide:protein mixtures were fitted using a three-exponentials decay model, having one of the time constants fixed at 1.2 ns. All of the curves fitted well to variable linear combinations of the fixed time constant decay, an additional decay with typical lifetimes of 2.2 ns, and a minor component with a longer lifetime on the order of 10 ns. The variations in relative amplitudes as a function of pigment:protein ratio (Figure 5) were in perfect agreement with the trends observed in the steady-state fluorescence measurements, reflecting the equilibrium between protein-bound and unbound ZnBChlide. Importantly, there is no indication for an additional component in HP7 complexes containing more than one ZnBChlide per protein. Given that the dead time of our TCSPC setup is 0.55 ns, this suggests that fluorescence quenching is due to a rapid relaxation channel for the excited state leading to lifetimes that are too short to be detected by our fluorescence lifetime setup.

Transient Absorption Spectroscopy. To investigate the dynamics of the rapid relaxation processes with subpicoseconds resolution, we recorded the transient absorption spectra of ZnBChlide:HP7 at 1:1 and 2:1 molar ratios in HEPES buffer. Component analysis of both samples resolved three decay-associated spectra (DAS) with typical lifetimes of 12 and 120 ps, and 2.7 ns (Figure 6A). All of the spectra shared similar features, particularly, a bleach of the Q_y absorption band at 760 nm and a broad excited-state absorption band with two peaks at 635 and 675 nm corresponding to $Q_y \rightarrow B_y$ and $Q_y \rightarrow B_x$ transitions, respectively. The contribution of each component to the decay kinetics differed significantly in the two samples:

dx.doi.org/10.1021/ja202054m |J. Am. Chem. Soc. 2011, 133, 9526–9535

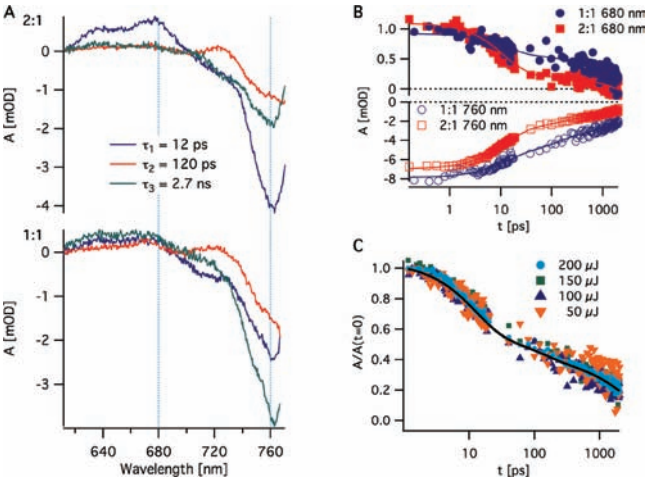

Figure 6. Component analysis of the transient absorption spectra of 1:1 and 2:1 ZnBChlide:HP7 complexes resolved three decay-associated spectra (DAS) with typical lifetimes of 12 and 120 ps and 2.7 ns; the shortest lifetime is predominant in the 2:1 complex (A, top), while the longest lifetime is predominant in the 1:1 complex (A, bottom). The recovery of bleached Q_y (760 nm) and the decay of excited-state absorbance (680 nm) were greatly accelerated in the 2:1 complex (B). The dynamics of the decay of excited-state absorbance at 680 nm was independent of laser power (C). The same trend was observed for the recovery of bleached Q_y (not shown).

while in the 1:1 ZnBChlide:HP7 sample the longest lifetime was predominant, the shortest lifetime predominated the 2:1 ZnBChlide:HP7 sample. Altogether, a dramatic acceleration of the relaxation kinetics in the 2:1 ZnBChlide:HP7 sample was revealed by comparing the recovery of bleached Q_y and the decay of excited-state absorbance (Figure 6B). The kinetics did not depend on laser power (Figure 6C), ruling out relaxation by singlet−singlet exciton annihilation processes. Apparently, the excitonic interactions between the HP7-bound couple of ZnBChlide molecules are the cause for the dramatic shortening of the singlet excited-state lifetime to 12 ps, about 200-fold shorter than the lifetime of a single HP7-bound pigment.

Triplet-State EPR and ENDOR Spectroscopy. The triplet-state EPR spectra of ZnBChlide complexes of HP7, HP7H7F, and HP7H42F at 1:1 molar ratios, as well as the 2:1 ZnBChlide:HP7 complex, were typical of a BChl triplet,[49] and essentially identical (Figure 7A), confirming that no excitonic delocalization of the triplet excited state occurs, which would essentially halve the width of the spectrum. The observation of an EPR signal per se also indicates that no excitation hopping takes place on time scales of or faster than the EPR experiment (faster than nanoseconds time scale). The slightly smaller *D* value of the 2:1 ZnBChlide:HP7 complex may be a consequence of increased order and stability due to occupying both HP7 binding sites with ZnBChlide.

To explore the differences between ZnBChlide:protein complexes in more detail, we used triplet-state ENDOR spectroscopy. Representative spectra recorded at three magnetic field settings are shown in Figure 7B−D. Two signals with large, positive and essentially isotropic couplings, 10.3 and 6.5 MHz, stem from the methyl protons at positions 2^1 and 12^1 (Scheme 1) [1].[49,50] In the ENDOR spectra recorded at positions C and D, a signal with a negative coupling constant (−2.4 MHz) can clearly be discerned. This signal likely stems from one of the methine

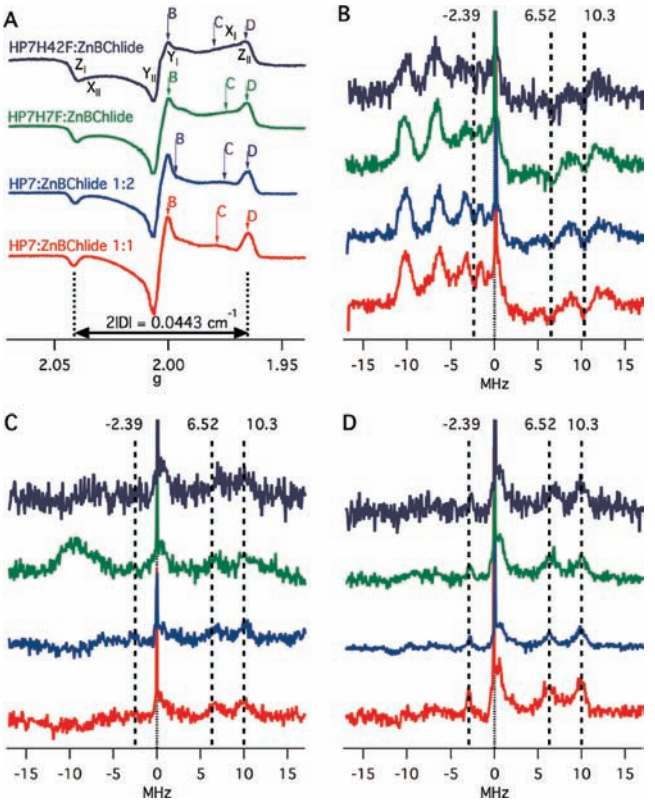

Figure 7. (A) Q-band ESE detected EPR spectra of ZnBChlide: HP7H42F, ZnBChlide:HP7H7F, and ZnBChlide:HP7 1:1 complexes, as well as ZnBChlide:HP7 2:1 complex recorded at 10 K. The zero field splitting parameter *D* amounts to 0.0222 cm^{-1}. The *E* parameter is essentially 0. (B-D) Davies ENDOR spectra for these four systems are shown for magnetic field settings B, C, and D. The ENDOR spectra allowed for identification of up to three signals, two with positive hyperfine coupling constants at 6.5 and 10.3 MHz and one with a negative coupling constant of −2.4 MHz.

protons at positions 5, 10, or 20 (Scheme 1).[49,50] Yet, even at the level of ENDOR spectroscopy, virtually no differences are observed between the different complexes. This indicates that the local protein environment of ZnBChlides at both binding sites is very similar, and incorporating ZnBChlide into one binding site has no effect on the environment at the other binding site.

DISCUSSION

HP7 is the best structurally and functionally characterized de novo designed heme-binding protein.[12,17,18] Critical to the success of this design, the result of more than a decade of iterative design and testing efforts,[13,14,51] is restricting the relative orientation of the four helices to a unique topology. This was achieved by a special loop arrangement that links the four helices in a monomeric "candelabra" fold (Scheme 2, **1**). In this arrangement, bis-histidine heme ligation between two parallel helix−loop−helix domains improves the stability of the syn conformation. The strong heme preference of bis-histidine ligation implies that HP7 is capable of binding up to two hemes per four-helix bundle. Replacing one histidine residue at position 7 or 42 with phenylalanine eliminates one heme-binding site. In contrast, ZnBChl derivatives almost exclusively prefer axial ligation by a single histidine.[20,26] Thus, an alternative binding conformation

Scheme 2. Possible Conformations for Heme and ZnBChlide Binding in HP7[a]

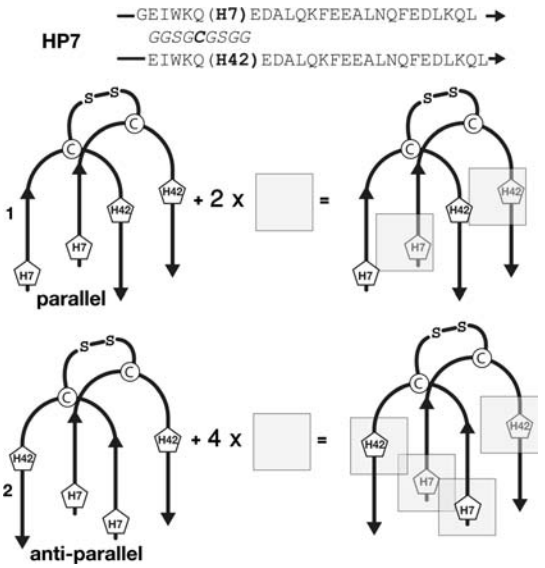

[a] Arrows mark single helix domains, pointing from the N to the C termini; S−S marks the disulfide bond between the cysteine residues of each polypeptide chain. The position of the cysteine residue is marked in bold on the helix−loop−helix sequence, and as a circle on the arrows diagram. The histidines at positions 7 and 42 are marked in bold on the helix−loop−helix sequence, and as pentagons on the arrows diagrams. The parallel conformation (**1**) is the only one possible for binding bis-histidine ligated heme; it is limited to only two heme-binding sites. ZnBChlide binding, which requires only one histidine ligand per pigment, is possible both in the parallel and in the anti-parallel (**2**) conformations, but in the latter, four histidines are available for ZnBChlide binding.

for ZnBChlide between antiparallel helix−loop−helix domains should be considered (Scheme 2, **2**). In this conformation, up to four histidines are available for ZnBChlide binding in HP7, and up to two in HP7H7F and HP7H42F. It is reasonable to assume that the GGSGCGSGG loop is flexible enough to allow rotation of the individual helices such that they form similar four-helix bundle cores in both the parallel and the antiparallel conformations. Our observations of specific binding by histidine ligation of a third ZnBChlide in HP7 and a second one in HP7H7F and HP7H42F are an indication for the presence of the antiparallel conformation. The lower affinity of these binding modes may suggest that the antiparallel conformation is unfavorable; however, pigment−pigment interactions due to steric crowding may also contribute to destabilizing these conformations. Although it is reasonable to assume, according to previous structural information of HP-type proteins,[13,18] that the parallel conformation prevails, more information is required to verify this assumption in the case of ZnBChlide binding.

BChl derivatives are excellent spectroscopic reporters of local molecular environment particularly due to their strongly absorbing and highly resolved Q_x and Q_y transitions. Protein−pigment and pigment−pigment interactions within the ZnBChlide complexes of HP7, HP7H7F, and HP7H42F result in distinctive CD and absorption spectra (Figure 2). These provide valuable information about the pigment organization within the protein core. In principle, this information should enable quantitative derivation of the relative orientations of bound ZnBChlide pigments;[52,53] yet, this requires a more rigorous analysis and additional measurements. Here, we derive a more qualitative picture from the trends in CD and absorbance spectra. The red shifts of the Q_x and Q_y absorption bands, a known indication of histidine ligation,[20−22] are the most obvious markers of binding ZnBChlide to the protein. These are essentially the same for all HP7 variants. Conversely, the CD and absorption spectra of interacting ZnBChlide molecules vary significantly in band position and lineshapes between HP7, HP7H7F, and HP7H42F. The variations in symmetry of the Q_x and Q_y CD bands of 2:1 ZnBChlide:HP7H7F and ZnBChlide:HP7H42F complexes are the most conspicuous and very informative (Figure 2A). The former is highly nonconservative, whereas the latter is more intense and conservative. Koolhaas et al.[52] have shown that in excitonically interacting BChl dimers, resonant coupling between two Q_x or two Q_y transitions leads to symmetric (conservative) CD bands around the respective transition energies, whereas nonresonant cross-coupling between these transitions results in asymmetric (nonconservative) CD. The overall CD spectra are, to a first approximation, linear combinations of the resonant and nonresonant coupling terms. The contribution of resonant coupling is usually predominant, but when the transition dipoles of the pigments lie on the same plane or at very small angles, nonresonant coupling becomes significant, increasing the nonconservative features of the CD spectrum.

The CD spectra suggest that the ZnBChlide macrocycles lie on the same plane in HP7H7F, but not in HP7H42F. This is reasonable considering the positions of binding histidines in each protein variant (Scheme 2) and that pigments are incorporated within the four-helix bundle core. The binding histidines in HP7H42F are at position 7, close to the N-terminal of each helix−loop−helix chain, whereas in HP7H7F these histidines are at position 42, close to the connecting loop in the middle of each chain. Consequently, the ZnBChlide pigments bound to HP7H42F are located in a region of the protein with more conformational flexibility than the ZnBChlide binding region of HP7H7F. The CD spectrum of 2:1 ZnBChlide:HP7 resembles but is not identical to the respective HP7H42F spectrum. Notably, the incorporation of the third ZnBChlide molecule changes the symmetry of the spectrum further by inverting the sign of the Q_x CD band. Given the spectral complexity and the number of possible binding conformations for 2:1 and 3:1 ZnBChlide:HP7 complexes, more rigorous analyses and simulations of the CD and absorption spectra are required to determine the actual conformation and relative orientations of the ZnBChlide molecules.

The formation of a ZnBChlide dimer within HP7 has a dramatic effect on the system's excited-state dynamics. The dimer's fluorescence is extremely quenched, and its quantum yield is reduced by about 80% as compared to the monomer. Time-resolved absorption spectroscopy reveals a reduction by 2 orders of magnitudes in singlet excited-state lifetime: from more than 2 ns in the monomeric species to 12 ps in the dimer. The independence of excited-state relaxation on light intensity and the static nature of the observed quenching process strongly suggest that the reduction of excited-state lifetime and fluorescence yield is the result of intramolecular interactions within the HP7-bound ZnBChlide dimer. In addition, the identical EPR and ENDOR spectra of dimeric and monomeric ZnBChlide species suggest that intersystem crossing predominates triplet formation and rules out any radical pair intermediate.[54] Thus, the rapid nonradiative relaxation of photoexcited ZnBChlide is most

likely due to excitonic interactions. Notably, the 100-fold reduction in excited-state lifetime is expected to quench 99% of the fluorescence signal. The observed 80% quenching and the multiexponential character of the time-resolved absorption signals are suggestive of several relaxation processes. This is probably due to the presence of a small population of HP7 proteins binding only a single ZnBChlide and/or conformational heterogeneity in the HP7-bound ZnBChlide dimer population.

The static and dynamic spectral properties of the HP7-bound ZnBChlide dimer match the description of the "statistical pair" that was introduced many years ago by Beddard and Porter[55,56] in their explanation of concentration quenching in dense solutions of Chls in polar solvents and lipid membranes. By definition, statistical pairs are the fraction of molecules in a statistical equilibrium distribution that are separated by less than a critical distance. Interactions between these molecules are most likely to provide rapid nonradiative relaxation channels for excited states, and thereby effective trapping of excitation energy that migrates through the system by resonance energy transfer. It was proposed, on the basis of these assumptions, that the role of proteins in LHCs is to avoid energy dissipation by keeping (B)Chl−(B)Chl separation longer than the critical distance that was estimated to be 1.0 nm in Chl solutions.[55,56] However, although analysis of recently available structures of natural (B)Chl proteins indicates that the mean (B)Chl−(B)Chl separation is indeed around 1.0 nm,[10,11,57] the general picture is more divergent and complicated. The most notable exception are the chlorosomes,[58] which contain only densely packed and highly ordered stacks of Chls, with no proteins at all, and yet are perfectly functional light harvesting systems. Clearly, pigment separation is not the only factor affecting the formation of quenching centers in natural LHCs. Unfortunately, very little is known about the mechanisms of excitation energy dissipation in (B)Chl−(B)Chl pairs, although it is widely accepted that relaxation involves a low-lying charge transfer state.[57,59] The key to functionality is probably controlling the energy levels of charge transfer states with respect to the excitonic states, which depends critically on the environment of the exciton-coupled pairs, their relative orientations, and interactions with the protein surroundings.[5]

In this context, the HP7 protein and its variants are extremely valuable model systems, being the first examples of a simple protein environment that can isolate a self-quenching pair of photosynthetic pigments in pure form. Unlike its complicated natural analogs, this system can be constructed from the ground up, starting with the simplest functional element, increasing the complexity as needed. Advances in computational protein design and our recent progress in understanding the unique factors that control pigment binding and organization in natural (B)Chl−protein complexes[25] provide us with the necessary tools for systematic variations of pigment orientations and protein environment. Furthermore, as we have demonstrated the excellent reporting properties of ZnBChlide absorption, CD, and fluorescence spectra provide immediate information about pigment assembly and organization within the protein, and their effect on excited-state dynamics. Constructing and characterizing such systems aimed at controlling the excited-state lifetime of (B)Chl pairs by manipulating (B)Chl−(B)Chl and protein−(B)Chl interactions is expected to teach us important lessons on the design principles of natural light energy harvesting systems. Particularly, such a system may be used to test whether a protein conformational change can act as a rapid switch between light harvesting and energy dissipation modes by turning on and off specific quenching centers between nearby pairs of (B)Chls[5,6] or (B)Chls and carotenoid.[60,61] Such a mechanism was suggested to be involved in the natural photoprotection process called "non-photochemical quenching" (NPQ),[62] but the lack of direct evidence for a conformational change in vivo[63,64] makes it highly controversial.[65] More generally, systematic studies of simple, controllable, and traceable protein−pigment systems may explain how slight variations in relative orientations and in the local environment can switch pairs of the same photosynthetic pigments from efficient light emitters to energy dissipaters in LHC or highly efficient photosensitizers of charge separation in RCs.

AUTHOR INFORMATION

Corresponding Author

dror.noy@weizmann.ac.il

Present Addresses

[§]Institut für Physikalische and Theoretische Chemie, Rheinische Friedrich-Wilhelms Universität Bonn, Bonn, Germany.

[‖]Group of Biological Physics, Institute of Physics, Polish Academy of Science, Warsaw, Poland.

ACKNOWLEDGMENT

D.N. acknowledges financial support from the Human Frontiers Science Program Organization's Career Development Award, and short-term fellowship, Israel Science Foundation individual grant, and the Weizmann Institute of Science's Center for New Scientists.

REFERENCES

(1) Holzwarth, A. R. In *Ultrashort Laser Pulses in Biology and Medicine*; Braun, M., Gilch, P., Zinth, W., Eds.; Springer: Berlin Heidelberg, 2008; pp 141−164.

(2) Wachtveitl, J.; Zinth, W. In *Chlorophylls and Bacteriochlorophylls*; Grimm, B., Porra, R. J., Rüdiger, W., Scheer, H., Eds.; Springer: Netherlands, 2006; Vol. 25, pp 445−459.

(3) Sundström, V. In *Photobiology*; Björn, L. O., Ed.; Springer: New York, 2008; pp 289−319.

(4) Cogdell, R. J.; Gardiner, A. T.; Hashimoto, H.; Brotosudarmo, T. H. P. *Photochem. Photobiol. Sci.* **2008**, *7*, 1150–1158.

(5) Müh, F.; Madjet, M. E. A.; Renger, T. *J. Phys. Chem. B* **2010**, *114*, 13517–13535.

(6) Müller, M. G.; Lambrev, P.; Reus, M.; Wientjes, E.; Croce, R.; Holzwarth, A. R. *ChemPhysChem* **2010**, *11*, 1289–1296.

(7) Cheng, Y.; Fleming, G. R. *Annu. Rev. Phys. Chem.* **2009**, *60*, 241–262.

(8) Renger, T.; Holzwarth, A. R. In *Biophysical Techniques in Photosynthesis*; Aartsma, T. J., Matysik, J., Eds.; Springer: Dordrecht, 2008; pp 421−443.

(9) van Grondelle, R.; Novoderezhkin, V. I. *Phys. Chem. Chem. Phys.* **2006**, *8*, 793–807.

(10) Noy, D. *Photosynth. Res.* **2008**, *95*, 23–35.

(11) Noy, D.; Moser, C. C.; Dutton, P. L. *Biochim. Biophys. Acta, Bioenerg.* **2006**, *1757*, 90–105.

(12) Anderson, J. L. R.; Koder, R. L.; Moser, C. C.; Dutton, P. L. *Biochem. Soc. Trans.* **2008**, *36*, 1106–1111.

(13) Huang, S. S.; Koder, R. L.; Lewis, M.; Wand, A. J.; Dutton, P. L. *Proc. Natl. Acad. Sci. U.S.A.* **2004**, *101*, 5536–5541.

(14) Koder, R. L.; Dutton, P. L. *J. Chem. Soc., Dalton Trans.* **2006**, *25*, 3045–3051.

(15) Shifman, J. M.; Moser, C. C.; Kalsbeck, W. A.; Bocian, D. F.; Dutton, P. L. *Biochemistry* **1998**, *37*, 16815–16827.
(16) Gibney, B. R.; Isogai, Y.; Rabanal, F.; Reddy, K. S.; Grosset, A. M.; Moser, C. C.; Dutton, P. L. *Biochemistry* **2000**, *39*, 11041–11049.
(17) Koder, R. L.; Anderson, J. L. R.; Solomon, L. A.; Reddy, K. S.; Moser, C. C.; Dutton, P. L. *Nature* **2009**, *458*, 305–309.
(18) Koder, R. L.; Valentine, K. G.; Cerda, J.; Noy, D.; Smith, K. M.; Wand, A. J.; Dutton, P. L. *J. Am. Chem. Soc.* **2006**, *128*, 14450–14451.
(19) Evans, T. A.; Katz, J. J. *Biochim. Biophys. Acta* **1975**, *396*, 414–426.
(20) Hartwich, G.; Fiedor, L.; Simonin, I.; Cmiel, E.; Schäfer, W.; Noy, D.; Scherz, A.; Scheer, H. *J. Am. Chem. Soc.* **1998**, *120*, 3675–3683.
(21) Noy, D.; Fiedor, L.; Hartwich, G.; Scheer, H.; Scherz, A. *J. Am. Chem. Soc.* **1998**, *120*, 3684–3693.
(22) Noy, D.; Yerushalmi, R.; Brumfeld, V.; Ashur, I.; Scheer, H.; Baldridge, K. K.; Scherz, A. *J. Am. Chem. Soc.* **2000**, *122*, 3937–3944.
(23) Yerushalmi, R.; Brandis, A.; Rosenbach-Belkin, V.; Baldridge, K. K.; Scherz, A. *J. Phys. Chem. A* **2006**, *110*, 412–421.
(24) Negron, C.; Fufezan, C.; Koder, R. L. *Proteins: Struct., Funct., Bioinf.* **2009**, *74*, 400–416.
(25) Braun, P.; Goldberg, E.; Negron, C.; von Jan, M.; Xu, F.; Nanda, V.; Koder, R. L.; Noy, D. *Proteins: Struct., Funct., Bioinf.* **2011**, *79*, 463–476.
(26) Lapouge, K.; Naveke, A.; Robert, B.; Scheer, H.; Sturgis, J. N. *Biochemistry* **2000**, *39*, 1091–1099.
(27) Razeghifard, A. R.; Wydrzynski, T. *Biochemistry* **2003**, *42*, 1024–1030.
(28) Mennenga, A.; Gärtner, W.; Lubitz, W.; Görner, H. *Phys. Chem. Chem. Phys.* **2006**, *8*, 5444–5453.
(29) Haehnel, W.; Noy, D.; Scheer, H. In *The Purple Phototrophic Bacteria*; Hunter, C. N., Daldal, F., Thurnauer, M. C., Beatty, J. T., Eds.; Springer: Dorderecht, 2008; Vol. 28, pp 895−912.
(30) Markovic, D.; Proll, S.; Bubenzer, C.; Scheer, H. *Biochim. Biophys. Acta, Bioenerg.* **2007**, *1767*, 897–904.
(31) Wright, K. A.; Boxer, S. G. *Biochemistry* **1981**, *20*, 7546–7456.
(32) Chen, M.; Eggink, L. L.; Hoober, J. K.; Larkum, A. W. D. *J. Am. Chem. Soc.* **2005**, *127*, 2052–2053.
(33) Dewa, T.; Yamada, T.; Ogawa, M.; Sugimoto, M.; Mizuno, T.; Yoshida, K.; Nakao, Y.; Kondo, M.; Iida, K.; Yamashita, K.; Tanaka, T.; Nango, M. *Biochemistry* **2005**, *44*, 5129–5139.
(34) Discher, B. M.; Noy, D.; Strzalka, J.; Ye, S.; Moser, C. C.; Lear, J. D.; Blasie, J. K.; Dutton, P. L. *Biochemistry* **2005**, *44*, 12329–43.
(35) Eggink, L. L.; Hoober, J. K. *J. Biol. Chem.* **2000**, *275*, 9087–9090.
(36) Kehoe, J. W.; Meadows, K. A.; Parkes-Loach, P. S.; Loach, P. A. *Biochemistry* **1998**, *37*, 3418–3428.
(37) Nagata, M.; Nango, M.; Kashiwada, A.; Yamada, S.; Ito, S.; Sawa, N.; Ogawa, M.; Iida, K.; Kurono, Y.; Ohtsuka, T. *Chem. Lett.* **2003**, *32*, 216–217.
(38) Noy, D.; Discher, B. M.; Rubtsov, I. V.; Hochstrasser, R. M.; Dutton, P. L. *Biochemistry* **2005**, *44*, 12344–54.
(39) Noy, D.; Dutton, P. L. *Biochemistry* **2006**, *45*, 2103–13.
(40) Omata, T.; Murata, N. *Plant Cell Physiol.* **1983**, *24*, 1093–1100.
(41) Brandis, A.; Mazor, O.; Neumark, E.; Rosenbach-Belkin, V.; Salomon, Y.; Scherz, A. *Photochem. Photobiol.* **2005**, *81*, 983–993.
(42) Laue, T.; Shaw, B. D.; Ridgeway, T. M.; Pelletier, S. L. In *Analytical Ultracentrifugation in Biochemistry and Polymer Science*; Harding, S. E., Rowe, A. J., Horton, J. C., Eds.; Royal Society of Chemistry: Cambridge, U.K., 1992; pp 90−125.
(43) Fisicaro, E.; Braibanti, A.; Lamb, J. D.; Oscarson, J. L. *Biophys. Chem.* **1990**, *36*, 1–14.
(44) Santosh, G.; Shirman, E.; Weissman, H.; Shimoni, E.; Pinkas, I.; Rudich, Y.; Rybtchinski, B. *J. Phys. Chem. B* **2010**, *114*, 14389–14396.
(45) Niklas, J.; Epel, B.; Antonkine, M. L.; Sinnecker, S.; Pandelia, M. E.; Lubitz, W. *J. Phys. Chem. B* **2009**, *113*, 10367–10379.
(46) Sinnecker, S.; Reijerse, E.; Neese, F.; Lubitz, W. *J. Am. Chem. Soc.* **2004**, *126*, 3280–3290.
(47) Connolly, J. S.; Samuel, E. B.; Janzen, A. F. *Photochem. Photobiol.* **1982**, *36*, 565–574.
(48) Connolly, J. S.; Janzen, A. F.; Samuel, E. B. *Photochem. Photobiol.* **1982**, *36*, 559–563.
(49) Lendzian, F.; Bittl, R.; Lubitz, W. *Photosynth. Res.* **1998**, *55*, 189–197.
(50) Marchanka, A.; Lubitz, W.; van Gastel, M. *J. Phys. Chem. B* **2009**, *113*, 6917–6927.
(51) Robertson, D. E.; Farid, R. S.; Moser, C. C.; Urbauer, J. L.; Mulholland, S. E.; Pidikiti, R.; Lear, J. D.; Wand, A. J.; Degrado, W. F.; Dutton, P. L. *Nature* **1994**, *368*, 425–431.
(52) Koolhaas, M. H. C.; vanderZwan, G.; vanMourik, F.; vanGrondelle, R. *Biophys. J.* **1997**, *72*, 1828–1841.
(53) Scherz, A.; Rosenbach-Belkin, V.; Fisher, J. R. E. In *Chlorophylls*; Scheer, H., Ed.; CRC Press: Boca Raton, FL, 1991; pp 237−268.
(54) Marchanka, A.; Savitsky, A.; Lubitz, W.; Mobius, K.; van Gastel, M. *J. Phys. Chem. B* **2010**, *114*, 14364–14372.
(55) Beddard, G. S.; Carlin, S. E.; Porter, G. *Chem. Phys. Lett.* **1976**, *43*, 27–32.
(56) Beddard, G. S.; Porter, G. *Nature* **1976**, *260*, 366–367.
(57) Beddard, G. S. *Philos. Trans. R. Soc., A* **1998**, *356*, 421–448.
(58) Ganapathy, S.; Oostergetel, G. T.; Wawrzyniak, P. K.; Reus, M.; Chew, A. G. M.; Buda, F.; Boekema, E. J.; Bryant, D. A.; Holzwarth, A. R.; de Groot, H. J. M. *Proc. Natl. Acad. Sci. U.S.A.* **2009**, *106*, 8525–8530.
(59) Yang, M.; Damjanovic, A.; Vaswani, H. M.; Fleming, G. R. *Biophys. J.* **2003**, *85*, 140–158.
(60) Ahn, T. K.; Avenson, T. J.; Ballottari, M.; Cheng, Y. C.; Niyogi, K. K.; Bassi, R.; Fleming, G. R. *Science* **2008**, *320*, 794–797.
(61) Pascal, A. A.; Liu, Z. F.; Broess, K.; van Oort, B.; van Amerongen, H.; Wang, C.; Horton, P.; Robert, B.; Chang, W. R.; Ruban, A. *Nature* **2005**, *436*, 134–137.
(62) Horton, P.; Ruban, A. *J. Exp. Bot.* **2005**, *56*, 365–373.
(63) Barros, T.; Kuehlbrandt, W. *Biochim. Biophys. Acta, Bioenerg.* **2009**, *1787*, 753–772.
(64) Barros, T.; Royant, A.; Standfuss, J.; Dreuw, A.; Kuhlbrandt, W. *EMBO J.* **2009**, *28*, 298–306.
(65) Cogdell, R. J. *Trends Plant Sci.* **2006**, *11*, 59–60.